ON THE CLUSTERING OF SUBMILLIMETER GALAXIES

Christina C. Williams[1], Mauro Giavalisco[1], Cristiano Porciani[2], Min S. Yun[1], Alexandra Pope[1], Kimberly S. Scott[3],
Jason E. Austermann[4], Itziar Aretxaga[5], Bunyo Hatsukade[6], Kyoung-Soo Lee[7], Grant W. Wilson[1], Ryan Cybulski[1],
David H. Hughes[5], Ryo Kawabe[6], Kotaro Kohno[8], Thushara Perera[9], and F. Peter Schloerb[1]

[1] Astronomy Department, University of Massachusetts, 710 North Pleasant Street, Amherst, MA 01003, USA; ccwillia@astro.umass.edu
[2] Argelander-Institut für Astronomie der Universität Bonn, Auf dem Hügel 71, D-53121 Bonn, Germany
[3] Department of Physics and Astronomy, University of Pennsylvania, 209 South 33rd Street, Philadelphia, PA 19104, USA
[4] Center for Astrophysics and Space Astronomy, University of Colorado, Boulder, CO 80309, USA
[5] Instituto Nacional de Astrofisica, Optica y Electronica (INAOE), Aptdo. Postal 51 y 216, 72000 Puebla, Pue., Mexico
[6] Nobeyama Radio Observatory, Minamimaki, Minamisaku, Nagano 384-1805, Japan
[7] Yale Center for Astronomy and Astrophysics, Department of Physics, Yale University, New Haven, CT 06520, USA
[8] Institute of Astronomy, the University of Tokyo, 2-21-1 Osawa, Mitaka, Tokyo 181-0015, Japan
[9] Department of Physics, Illinois Wesleyan University, Bloomington, IL 61701, USA

ABSTRACT

We measure the angular two-point correlation function of submillimeter galaxies (SMGs) from 1.1 mm imaging of the COSMOS field with the AzTEC camera and ASTE 10 m telescope. These data yield one of the largest contiguous samples of SMGs to date, covering an area of 0.72 deg^2 down to a 1.26 mJy beam^{-1} (1σ) limit, including 189 (328) sources with S/N $\geqslant$ 3.5 (3). We can only set upper limits to the correlation length r_0, modeling the correlation function as a power law with pre-assigned slope. Assuming existing redshift distributions, we derive 68.3% confidence level upper limits of $r_0 \lesssim$ 6–8h^{-1} Mpc at 3.7 mJy and $r_0 \lesssim$ 11–12 h^{-1} Mpc at 4.2 mJy. Although consistent with most previous estimates, these upper limits imply that the real r_0 is likely smaller. This casts doubts on the robustness of claims that SMGs are characterized by significantly stronger spatial clustering (and thus larger mass) than differently selected galaxies at high redshift. Using Monte Carlo simulations we show that even strongly clustered distributions of galaxies can appear unclustered when sampled with limited sensitivity and coarse angular resolution common to current submillimeter surveys. The simulations, however, also show that unclustered distributions can appear strongly clustered under these circumstances. From the simulations, we predict that at our survey depth, a mapped area of 2 deg^2 is needed to reconstruct the correlation function, assuming smaller beam sizes of future surveys (e.g., the Large Millimeter Telescope's 6$''$ beam size). At present, robust measures of the clustering strength of bright SMGs appear to be below the reach of most observations.

Key words: galaxies: evolution – galaxies: high-redshift – large-scale structure of universe – submillimeter: galaxies

1. INTRODUCTION

High-redshift galaxies which are relatively bright at millimeter and submillimeter wavelengths, and thus detectable by current ground-based instrumentation, have, over the last decade, come to the forefront of studies of galaxy evolution. Commonly referred to as submillimeter galaxies (SMGs), because the first significant deep surveys have been made at λ = 450 and 850 μm, these sources are thought to be largely obscured by dust, with star formation rates of up to 1000 $M_\odot$ year^{-1} needed to power their high rest-frame infrared luminosity of $L_{\rm IR} \sim 10^{12}$–10^{13} $L_\odot$ (Smail et al. 1997; Hughes et al. 1998; Barger et al. 1998). It has long been speculated that with such high luminosity and star formation rates, SMGs should be very massive, strongly clustered, and trace large-scale structure at high redshift (Blain et al. 2004; Amblard et al. 2011). If it is conclusively found that SMGs do cluster strongly in space, and therefore trace massive dark matter halos at high redshift, this will provide additional evidence that these sources are evolutionarily linked to massive elliptical galaxies often found in the center of galaxy clusters in the local universe (Lilly et al. 1999; Eales et al. 1999). Hence, robust determination of the clustering strength of the SMGs, at least of those that are commonly detected with current instrumentation, namely, with flux brighter than a few mJy, would have strong implications in theories of galaxy evolution (van Kampen et al. 2005; Negrello et al.

2007), as it is not well understood what observable properties of galaxies are characteristic of biased tracers of the background dark matter distribution.

Until recently, a secure measurement of SMG clustering has been elusive (Webb et al. 2003; Blain et al. 2004; Scott et al. 2006; Weiß et al. 2009), in large part because of the slow mapping speeds of submillimeter instruments, whose maps have been very small in area. Recently, data at 250–500 μm from the *Herschel Space Telescope* have produced improvements in terms of the area of submillimeter maps, allowing clustering measurements to be made with improved statistics (Maddox et al. 2010; Cooray et al. 2010). The *Herschel* surveys, however, are biased to low-redshift and low-luminosity galaxies as a result of the bluer wavelengths that they cover and of the negative *k*-correction; they also still suffer from source confusion despite their large area. Clustering measurements at longer wavelengths, on the other hand, still remains uncertain. Submillimeter surveys are still limited by large beam size and shallow survey depths which have prevented robust positions and large sample sizes. As submillimeter maps become larger with higher resolution, and the number of securely detected sources becomes statistically significant, studies of clustering of these SMGs will surely provide interesting implications for galaxy evolution.

Here, we present measures of the angular clustering of SMGs from one of the first millimeter maps containing a statistically
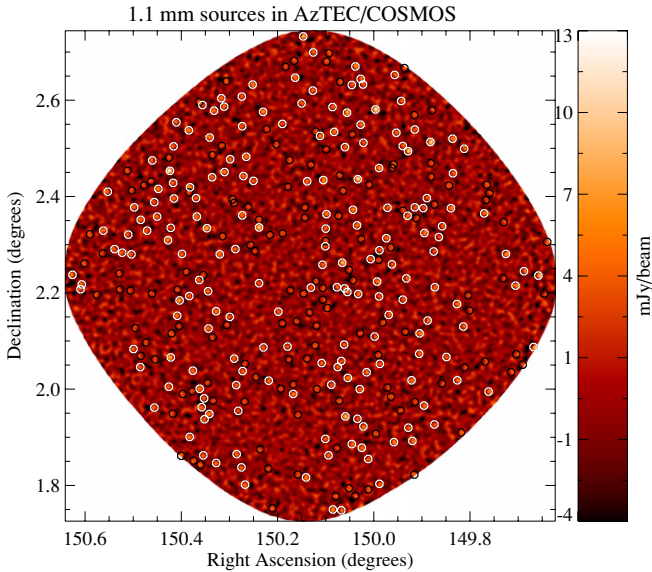
Figure 1. 50% coverage region in the AzTEC/COSMOS map. 3.0 to 3.5σ sources are circled in black, >3.5σ sources are circled in white. Circle size corresponds to one and a half times the beam size.

significant number of SMGs. This map covers a 1 deg^2 section of the Cosmic Evolution Survey (COSMOS; Scoville et al. 2007) field using the AzTEC bolometer array, mounted on the Atacama Submillimeter Telescope Experiment (ASTE). The data provide the largest contiguous map, and the largest galaxy sample, at 1.1 mm to date (I. Aretxaga et al. 2011, in preparation). While spectroscopic redshift information on SMGs remains sparse, we have used various redshift distributions to estimate de-projected spatial clustering for these galaxies. We assume a cosmology with $\Omega_\Lambda = 0.7$, $\Omega_m = 0.3$, and $H_o = 100\, h\, \mathrm{km\, s^{-1}\, Mpc^{-1}}$.

2. OBSERVATIONS

The COSMOS field was mapped with AzTEC on ASTE, a full description and results will be presented in a separate publication (I. Aretxaga et al. 2011, in preparation). We imaged a subset of the COSMOS blank field centered at (R.A., Decl.) = (150.125, 2.23) with a total area of 1.41 deg^2, totaling 112.6 hr of observing time. With AzTEC on ASTE, the beam size is 28″ (full width at half-maximum). For this analysis we have considered only the region of the map where the coverage was 50% of the maximum value or higher. This results in a contiguous map of 0.72 deg^2. We achieve an average noise level of 1.26 mJy beam^{-1}, which is very uniform throughout the area considered, ranging from 1.23 to 1.27 mJy beam^{-1}.

Our millimeter sources are selected by searching for peaks above a given signal-to-noise ratio (S/N) with a window corresponding to the beam size (e.g., Scott et al. 2008). We find 328 sources with an S/N above 3.0, and 189 sources with an S/N above 3.5, hereafter the 3.0σ and 3.5σ catalogs, respectively. The map and source positions are shown in Figure 1.

3. CLUSTERING ANALYSIS

3.1. Angular Clustering

The angular two-point correlation function, $w(\theta)$, measures the excess probability, above that expected for a random distribution, of finding two galaxies with an angular separation θ, within a solid angle $\delta\Omega$. It is defined in terms of the probability
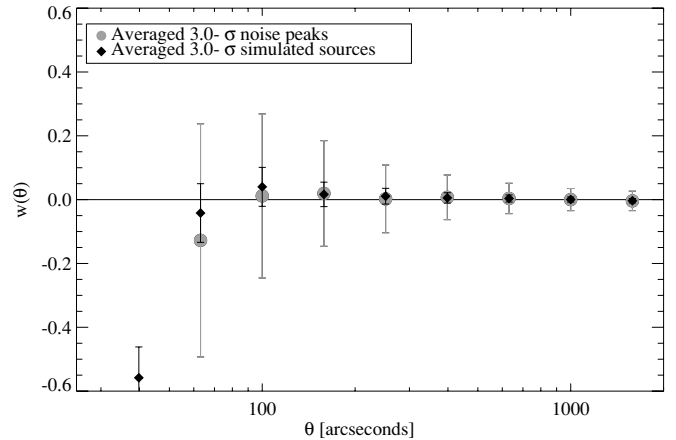

Figure 2. Averaged ACF for the peaks detected at 3.0σ from the 100 noise realizations (gray circles) and for the simulated sources detected at 3.0σ (black diamonds). Errors indicate standard deviation. Gray horizontal line corresponds to zero clustering. Slight anticorrelation around the 60″ bin is a result of the beam size; in general more random pairs with angular separations in this bin will be found since distances between detected sources are not smaller than twice the beam size.

$\delta P = N^2[1 + w(\theta)]\delta\Omega$, where N is the surface density of galaxies (Peebles 1980). We measure angular clustering of SMGs in the COSMOS field using the Landy–Szalay estimator of the angular correlation function (ACF; Landy & Szalay 1993). This can be measured as

$$w(\theta) = \frac{DD(\theta) - 2DR(\theta) + RR(\theta)}{RR(\theta)},$$

where $DD(\theta)$ is the number of observed galaxy pairs as a function of angular separation, θ, $DR(\theta)$ are the number of cross-pairs between the observed galaxies and a randomly distributed sample, and $RR(\theta)$ is the number of randomly distributed pairs. The random distributions are generated by inserting randomly positioned sets of artificial sources into realizations of the noise distribution in our COSMOS map. The injected sources have a flux distribution based on our best estimate of SMG number counts from blank field observations (Austermann et al. 2010), but we tuned the parameters such that the number of significant sources retrieved by our source finding algorithm are on average within 2% of the number of detections in the real map. We generate 100 of these simulations, and we use the random sources selected above the corresponding S/N threshold from each as random distributions. We have verified that (on average) the noise peaks in our COSMOS map and sources in the simulations are unclustered at the angular separations we consider (see Figure 2).

We expect our uncertainty to be dominated by small number statistics, but it is possible that the map properties, such as non-uniformity and beam size, contribute to our error in measuring the ACF. So rather than assume Poisson errors[10] given by $\delta w(\theta) = \frac{1+w(\theta)}{\sqrt{DD(\theta)}}$ (Landy & Szalay 1993), which do not take these effects into account, we also quantify the uncertainty using the simulations. To do this we calculate the ACF of each of the 100 simulated random catalogs, whose intrinsic ACF we know (on average we found that simulated sources are unclustered). Thus, the standard deviation of the ACF of the

---

[10] We found that Poisson errors are sometimes incorrectly used in the literature, as $\delta w(\theta) = \sqrt{\frac{1+w(\theta)}{DD(\theta)}}$. The correct expression is $\delta w(\theta) = \frac{1+w(\theta)}{\sqrt{DD(\theta)}}$ (Landy & Szalay 1993).
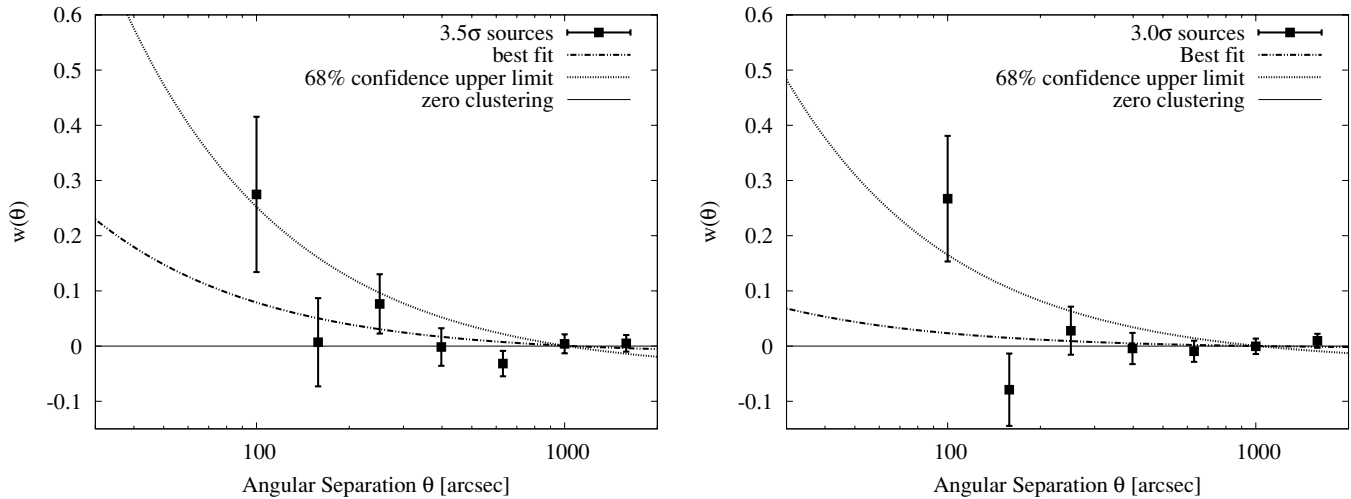
Figure 3. ACF for the two catalogs (points). The lower dot-dashed lines are the best-fit power law to the data, upper dotted lines are the 68.3% confidence level upper limits. Both power laws shown assume $\beta = 0.8$ and have their corresponding IC subtracted to match what is fit to the data.

individual simulated catalogs, $\sigma_{\rm sim}(\theta)$, should include any error in $w(\theta)$ related to the properties of the map. This uncertainty is given by $\delta w(\theta) = (1 + w(\theta))\sigma_{\rm sim}(\theta)$. We find the uncertainty obtained this way to be smaller than the Poissonian error for both catalogs, so we have conservatively assumed the latter.

The difference between the 3.0σ and 3.5σ catalogs from the observed map is a trade off between a larger catalog of galaxies, and a lower false detection rate of sources in our observed map. By setting a high S/N threshold for detection we can achieve negligible false detections, but our number of sources would be small. We choose to select sources with a lower S/N threshold, while acknowledging that some fraction of them are not real SMGs. For the 3.5σ catalog, we expect that about 9% of the sources are false detections, and for the 3.0σ catalog, 24% are false detections (I. Aretxaga et al. 2011, in preparation). Including some fraction of randomly positioned non-galaxies will only serve to dilute our estimate of the clustering. As noise peaks are inherently unclustered, we can correct for this effect as $w_{\rm obs}(\theta) = (1 - f)^2 w_{\rm true}(\theta)$, where f is the fraction of false detections included in the catalog. Our ACF estimate, corrected for dilution by random false detections, is presented in Figure 3. We do not include in the analysis ACF measurements at angular separations smaller than twice the beam size.

We assume that at the angular separations we are considering, the ACF behaves as a power law of the form $w(\theta) = A_w\theta^{-\beta} -$ IC, where we refer to A_w as the clustering amplitude. IC refers to the integral constraint correction, which we calculate using the algorithm of Roche & Eales (1999). The result of a power-law fit where the clustering amplitude and slope β are left as free parameters is poorly constrained, and the best slope is unphysically steep due to the fact that the measured ACF is high at the lowest angular scale. So given our large uncertainties, we do not attempt to constrain both clustering amplitude and slope. Instead, we assume two different representative values for β. The first, $\beta = 0.8$, is observed for massive elliptical galaxies in large low-redshift surveys and is the value typically assumed for massive galaxies and SMGs at high redshift (Zehavi et al. 2002; Blain et al. 2004). The second value, $\beta = 0.6$, is the shallower slope typically observed for normal ultraviolet-selected starbursting galaxies at high redshifts such as Lyman break galaxies (LBGs) and BX/BM galaxies (Giavalisco & Dickinson 2001; Porciani & Giavalisco 2002; Lee et al. 2006;

Adelberger et al. 2005), as well as star-forming galaxies at low redshift (Zehavi et al. 2002). Unless otherwise stated, in the text we will quote results derived using $\beta = 0.8$.

In Figure 3, we also show the best-fitting power laws (assuming $\beta = 0.8$) for each catalog found from a least-squares minimization. Due to the large uncertainties, the best-fit amplitudes are poorly constrained and the 1σ upper limits to these best-fit values are large. These upper limits are also shown in Figure 3. The case of zero clustering lies within the 1σ error (defined as $\Delta\chi^2 < 1$), but as negative values imply anticorrelation and are considered unphysical, we set zero clustering to be the lower limit. These best fits, 1σ upper error, and lower error (as described above) are $A_w = 3.7^{+8.2}_{-3.7}$ arcsec$^{0.8}$ for the 3.5σ catalog and $A_w = 1.1^{+6.7}_{-1.1}$ arcsec$^{0.8}$ for 3.0σ, and are summarized in Table 1 along with results assuming $\beta = 0.6$.

While this χ^2 analysis provides a best fit with confidence intervals, it does not limit a priori the possible range of values that A_w can assume. We want to explore the effect on the power-law fit if we only consider positive values for A_w, as negative values are unphysical. To do this we perform Monte Carlo simulations where we generate 5000 Gaussian deviated realizations of the observed ACF. The Gaussian deviates are generated using the Poisson error on each value of $w(\theta)$. We fit each deviated realization with the same power-law form outlined above to produce a distribution of best-fitting clustering amplitudes, A_w. The resulting distributions in A_w, given assumed values of β, are shown for each catalog in Figure 4. For both catalogs, the most likely values to be measured for A_w is zero, corresponding to the case where SMGs are unclustered. It must be emphasized that this does not mean that SMGs such as these are spatially unclustered, only that the strength of their clustering is below what is robustly detectable from our survey. The peak at zero is merely an effect of the likelihood of the χ^2 distribution extending into the negative values of A_w, since A_w is poorly constrained.

Using these distributions shown in Figure 4, we set upper limits to the power-law amplitudes which are allowable given our measured ACF for SMGs, so our results can be compared with previous measurements of SMG clustering. These distributions are one-sided (because the peak lies at zero, the lowest value we allow for A_w), and so the distributions can only provide an upper limit. This is in contrast to the χ^2 distribution which is two-sided

Table 1
SMG Clustering Results

Catalog	N	S^a (mJy)	Fit Type[b]	β	$A_w{}^c$ Best	$A_w{}^c$ Upper Limit	IC^d	$r_o{}^e$ Best	$r_o{}^e$ Upper Limit	$r_o{}^f$ Best	$r_o{}^f$ Upper Limit
3.5σ	189	4.2	χ^2_ν	0.8	3.7	11.9	0.015	10.0	19.2	9.6	18.4
				0.6	1.2	4.4	0.018	9.5	21.4	9.0	20.4
			MC 68.3%	0.8		5.2			12.1		11.6
				0.6		1.8			12.2		11.7
			MC 99.5%	0.8		11.5			18.8		18.1
				0.6		4.3			21.1		20.1
3.0σ	328	3.7	χ^2_ν	0.8	1.1	7.8	0.004	5.1	15.2	4.7	14.6
				0.6	0.3	2.9	0.004	4.0	16.5	3.8	15.7
			MC 68.3%	0.8		2.4			7.9		7.6
				0.6		0.7			6.8		6.5
			MC 99.5%	0.8		7.9			15.3		14.7
				0.6		2.8			16.1		15.4

Notes.
[a] Flux limit at 1.1 mm of the catalog.
[b] For the reduced χ^2 fit, best-fitting results are listed with the corresponding upper limit where $\Delta\chi^2_\nu > 1$. In the case of the Monte Carlo results (indicated by MC), values are percentages of confidence level upper limit in the acceptable value of amplitude A_w, given the SMG catalog.
[c] Best fits and upper limits to A_w (in arcseconds$^\beta$). Lower limits in all cases are zero as explained in the text.
[d] IC values correspond to the best-fit power law.
[e] Correlation length in units h^{-1} Mpc, given our assumption of redshift distribution of Chapman et al. (2005).
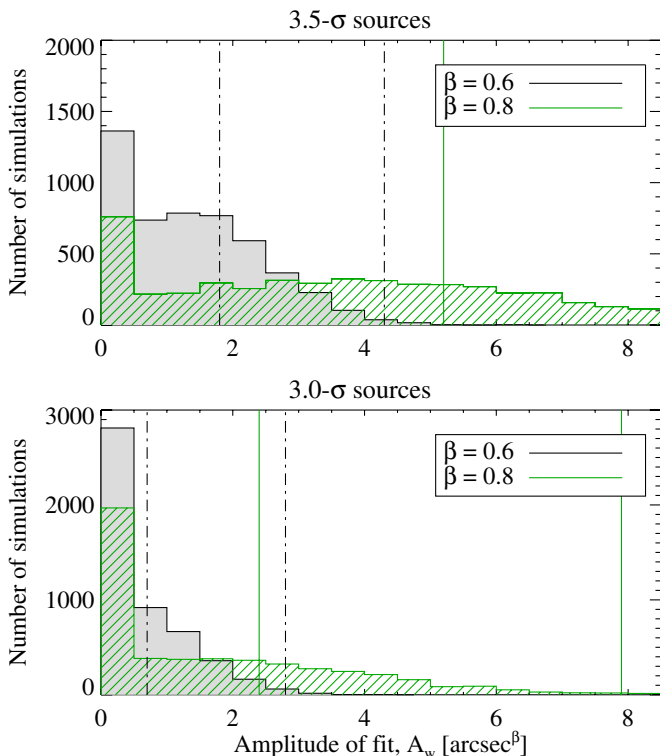[f] Using redshift distribution of Chapin et al. (2009).

Figure 4. Distributions in amplitudes for power-law fits with slopes fixed to $\beta = 0.8$ and 0.6 for 3.0σ and 3.5σ catalogs, generated by Monte Carlo simulations of the observed ACF. The vertical lines correspond to the 68.3% (smaller A_w) and 99.5% (larger A_w) limits in each distribution and represent the largest clustering strengths allowable by our data sets. See Table 1 for corresponding values.

and so provides an upper and a lower limit (where conventionally the 68.3% confidence limits are given by $\Delta\chi^2 < 1$). The two upper limits are different from each other in that the 68.3% confidence level upper limit from the χ^2 minimization corresponds to a 15.85% probability of finding a larger A_w, whereas the one-sided 68.3% confidence level upper limit from the Monte Carlo simulation corresponds to a 31.7% probability of finding a larger A_w. We find that using these distributions from the Monte Carlo simulations we can reject power-law models with amplitudes larger than $A_w = 2.4$ arcsec$^{0.8}$ at the 68.3% confidence level, and $A_w = 7.9$ arcsec$^{0.8}$ at the 99.5% confidence level for the 3.0σ catalog, and $A_w = 5.2$ and $A_w = 11.5$ arcsec$^{0.8}$ at the 68.3% and 99.5% confidence levels, respectively, for the 3.5σ catalog. These results are shown as solid and dashed vertical lines in Figure 4 and are summarized in Table 1.

3.2. Spatial Clustering

To derive the spatial correlation length we have de-projected the ACF using the Limber transformation (Peebles 1980) and assuming a redshift distribution for SMGs. Robust measures of this distribution are limited in large part because coarse angular resolution of submillimeter and millimeter maps results in large positional uncertainties, making counterpart identification for spectroscopic followup difficult. The crude knowledge of the redshift distribution for these galaxies provide an additional source of systematic error in the derivation of the spatial clustering. Here, we discuss results obtained by assuming two redshift distributions which are believed to be representative of SMGs detected in the same range of far-IR wavelengths as the ones considered here. The most widely used is the distribution of Chapman et al. (2005), compiled from a set of 75 spectroscopic redshifts for $850\,\mu$m selected SMGs with optical counterparts identified using deep interferometric radio continuum imaging. This redshift distribution is known to be biased toward low redshifts due to the requirement of a radio detected counterpart, so we use the version of this distribution which has been corrected for the radio bias. The corrected distribution is well described by a Gaussian peaking at $z = 2.3$ and a spread of 1.2, ranging from $1 < z < 3.5$. Using this distribution, we find that the 68.3% confidence level upper limits of consistent correlation

lengths for SMGs are $\lesssim 6$–$8\ h^{-1}$ Mpc and $\lesssim 11$–$12\ h^{-1}$ Mpc for the 3.0σ and 3.5σ catalogs, respectively. Results assuming the redshift distribution of Chapin et al. (2009) produce similar values, which are summarized in Table 1. The Chapin et al. (2009) redshift distribution is generated from a combination of spectroscopic and photometric redshifts for 1.1 mm detected galaxies, and so may be more applicable to this study. The distribution differs from that of Chapman et al. (2005) in that it peaks around $z = 2.7$ and has a high-redshift tail to $z \gtrsim 4$. We emphasize that these results are upper limits, and therefore the intrinsic clustering of this set of galaxies are likely to be lower.

4. DISCUSSION

4.1. Comparison to Other SMG Clustering Measurements

Before comparing our clustering measures with other works it is important to keep in mind the limitations inherent in the selection of samples based on an observable property, such as flux, as opposed to a physical property, such as luminosity or mass. The term "submillimeter galaxies" is often used to indicate a category of galaxies (population is the term often used in this context) thought to have well specified and somewhat homogeneous properties. For example, SMGs are commonly interpreted as massive systems characterized by prodigious star formation rates powered by major merger events. While these properties most likely apply to *some* SMGs of relatively large far-IR luminosity, it obviously is unreasonable to think that they are generic to *any* galaxy that is detectable at some wavelengths around 1 mm. First, we should remind that galaxies detected at some wavelength with some telescope/instrument combination do not, generally speaking, span the same range of the far-IR luminosity function or redshift as galaxies from another instrumental configuration observed at another wavelength in the submillimeter/millimeter spectral region. Lumping all such samples as "SMG" believing that they share very similar properties is misleading. In other words, the definition of "SMG" as galaxies that are detected at wavelengths crudely in the range $500\ \mu$m to 1 mm at the sensitivity of current survey facilities does not result into the selection of common physical properties. It is true that, since current ground-based facilities working at the popular $850\ \mu$m wavelength have limited dynamic range in sensitivity, the resulting samples of galaxies at similar redshifts also have similar far-IR luminosity and thus, presumably, physical properties. But this is just an "observational accident" that does not apply to other submillimeter surveys. In general, galaxies detected at $350\ \mu$m with *Herschel*/SPIRE or at 1.1 mm with ASTE/AzTEC, even if at the same redshift as those observable with the James Clerk Maxwell telescope (JCMT)/SCUBA, will cover different portion of the far-IR luminosity function, and will generally have different physical properties, such as mass, clustering strength, star formation rate, etc. (we are not addressing here the different sensitivity and redshift distribution function of the corresponding samples).

With this caveat in mind, we can try to compare our results with others. We find that at 1.1 mm and down to 1.26 mJy the angular clustering of SMGs in the COSMOS field is poorly constrained and with our sample size we can only set upper limits to the correlation length. Our 68.3% confidence level upper limits to the correlation length from the Monte Carlo simulation are $\lesssim 6$–$8\ h^{-1}$ Mpc or $\lesssim 11$–$12\ h^{-1}$ Mpc, depending on flux limit. Generally, our SMG clustering limits are higher for the higher flux limit (4.2 mJy). The recent prediction from the theoretical model of SMG clustering by Almeida et al. (2010) for
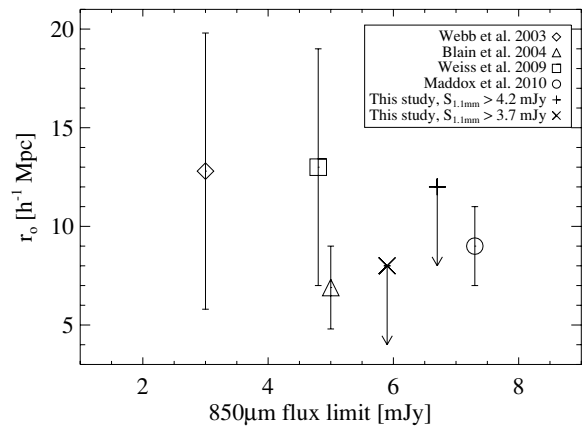

Figure 5. Correlation lengths and flux limits (translated to $850\ \mu$m using the spectral index of Chapin et al. 2009) from this and previous studies.

$S_{850\,\mu m} > 5$mJy is $r_o \sim 5\ h^{-1}$ Mpc, which is consistent within the error of our measurements. The $S_{1.1\,mm} > 3.7$Jy flux limit of the 3.0σ sources roughly translates to $S_{850\,\mu m} > 5.9$mJy, assuming the spectral index suggested by Chapin et al. (2009) of $S_\nu \propto \nu^{1.8}$ between 1.1 mm and $850\ \mu$m sources. Our 1.1 mm sources are likely similar to this simulated galaxy distribution.

In terms of the results of previous studies of SMG clustering, direct comparisons are difficult to make because of the differing wavelengths and flux limits of each survey. Poorly quantified redshift distributions in all cases further complicate the issue when trying to make comparisons. As we found in this paper, the brighter SMGs show evidence for stronger clustering than the fainter SMGs consistent with what is expected from galaxy evolution models (e.g., Almeida et al. 2010). A similar result is also found by Brodwin et al. (2008) based on the clustering of *Spitzer*-selected ultraluminous infrared galaxies. This demonstrates that caution should be taken when comparing the clustering of different samples of SMGs selected at different wavelengths down to different depths. If we ignore these effects, a direct comparison makes our upper limits inconsistent with the results of Scott et al. (2006), but consistent with the majority of other previous studies due to large uncertainties which tend to be larger than 20%–50% in r_o (Webb et al. 2003; Blain et al. 2004; Weiß et al. 2009; Maddox et al. 2010). These comparisons are summarized in Table 2 and Figure 5. Our flux limit is generally higher than other studies, when translated to a common wavelength, so it may be reasonable to assume that the AzTEC sources should be more strongly clustered.

In a recent paper, Amblard et al. (2011) measured the clustering at 250–$500\ \mu$m from the brightness fluctuations in the power spectrum of *Herschel*/SPIRE maps after masking out the bright, detected sources. Assuming we are probing the Raleigh–Jeans tail of the spectral energy distribution, the average flux density ratio is $S_{1.1\,mm}/S_{350\,\mu m} \sim 8$ (with a spectral index of 1.8; Chapin et al. 2009). Given the confusion limit of SPIRE, these fluctuations are probing the clustering of sources down to $350\ \mu$m fluxes of a few mJy (Amblard et al. 2011), which translates to only 0.4 mJy and 0.25 mJy at $850\ \mu$m and 1.1 mm, respectively. This limit probes galaxies down to $L_{\rm IR} \sim 3 \times 10^{11}\ L_\odot$ at $z \sim 2$, much fainter than the typical limits of submillimeter surveys. It is not clear which part of the far-IR luminosity function contributes most to the clustering signal measured by the fluctuations.

Table 2
SMG Clustering and Flux Limits

$N_{sources}$	$r_o \pm \delta r_o$ (h^{-1} Mpc)	λ (μm)	S_ν (mJy)	$S_{850\,\mu m}$ (mJy)	Beam Size (arcsec)	Reference
27	12.8 ± 7.0	850	3.0	3.0	14.5	Webb et al. (2003)
47	6.9 ± 2.1	850	5.0	5.0	14.5	Blain et al. (2004)
51	31[a]	850	5.0	5.0	14.5	Scott et al. (2006)
126	13 ± 6	870	4.6	4.8[b]	19.2	Weiß et al. (2009)
1633	7–11	350	36	7.3[b]	17	Maddox et al. (2010)
189	<11–12[c]	1100	4.2	6.7[b]	28	This study
328	<6–8[c]	1100	3.7	5.9[b]	28	This study

Notes.
[a] Only angular clustering was published by Scott et al. (2006); we transform their power-law result and errors for their sources above S/N of 3.5, using the redshift distribution of Chapman et al. (2005).
[b] Flux density translated assuming $S_\nu \propto \nu^{1.8}$.
[c] We have quoted our 68.3% confidence level upper limits for comparison.

While the Amblard et al. (2011) result provides an interesting constraint on the clustering of fainter submillimeter-emitting galaxies, these sources are much more numerous than typical SMGs (e.g., Smail et al. 2002) and are not expected to evolve into the most massive elliptical galaxies in the local universe. The halo masses derived in Amblard et al. (2011) are more comparable to those of the less extreme Lyman break galaxies than the bright, detected SMGs. With larger telescopes such as the Large Millimeter Telescope (LMT) and Cerro Chajnantor Atacama Telescope (CCAT), we will be able to individually detect galaxies down to $S_{1.1\,mm} < 0.1$ mJy and measure the clustering as a function of luminosity, a strong test of various galaxy evolution models.

The strength of SMG clustering is an additional test of evolutionary models because it can discriminate between the various formation mechanisms for SMGs. Discriminating between merging or cold-mode accretion as the dominant mechanism by which SMGs form at high redshift is of particular interest, and recent simulations of each mechanism predict different correlation lengths. The model of Davé et al. (2010), where SMGs are formed by accretion of large amounts of cold gas, predicts a large correlation length ($r_o \sim 10\,h^{-1}$ Mpc) because cold gas accretion should be most influential in the most massive dark matter halos. Merger driven scenarios on the other hand predict a more modest range in correlation lengths, between $r_o = 5$ and $6\,h^{-1}$ Mpc (Almeida et al. 2010). We are not yet at the point where we can see distinguishing evidence between the models, but this will also be an important goal of larger submillimeter observatories.

Additionally, due to the large uncertainty in our measurement, our results are also consistent with measurements of weaker clustering from other types of high-redshift star-forming galaxies such as LBGs and other rest-frame UV-selected galaxies, BzKs, and unresolved sources contributing to the cosmic infrared background (Lee et al. 2006; Adelberger et al. 2005; Giavalisco & Dickinson 2001; Hayashi et al. 2007; Viero et al. 2009). Their minimum halo masses of $\sim 10^{11}$–$10^{12}\,M_\odot$ and correlation lengths of about $r_0 \sim 4$–$5\,h^{-1}$ Mpc (Lee et al. 2006; Porciani & Giavalisco 2002; Adelberger et al. 2005) are consistent with the masses and correlation lengths for both bright and faint SMGs (Almeida et al. 2010; Amblard et al. 2011). If the underlying submillimeter galaxy population we detected in this study is weakly clustered, as may be implied by Almeida et al. (2010) and Amblard et al. (2011), it supports our conclusion from Section 2 that the clustering is too weak to be detected with our survey.

4.2. Map Limitations on Measuring Clustering

From a practical point of view, an important question to answer is: what characteristics of area and depth should surveys of SMGs have in order to yield robust measures of clustering. For example, how much area and down to which flux limit should a survey with AzTEC reach in order to test the hypothesis that SMGs at the bright end of the far-IR luminosity function are the progenitors of massive elliptical galaxies, and should therefore be strongly clustered? In addressing this question, one needs to take into account the key contributors to the error budget of the measures, such as (1) the uncertainty in the redshift distribution, since a wide one that covers a large redshift interval washes out the clustering signal due to projection effects; (2) the sparse sampling of the underlying SMG population, which determines the shot noise in the ACF measures; and (3) the large beam size of current observations, which prevents one from measuring the ACF at small angular scales where the signal is strongest.

We have done Monte Carlo simulations to investigate the extent to which these map properties are affecting our ability to measure SMG clustering. Specifically, we measure the ACF from realizations of galaxy distributions for which we have defined the intrinsic clustering and impose AzTEC-like map properties. The realizations are made by generating a log-normal density distribution with an intrinsic ACF and Poisson sampling the density field according to the methods outlined in Porciani & Giavalisco (2002). The resulting realizations are $0.72\,deg^2$ in area and contain on the order of 10^4 mock galaxies. To match the expected percentage of false detections, we merge the clustered mock set with a set of random positions, so that they make up 9%, like the 3.5σ catalog. We then randomly sample points from the realization to match the observed number density of 3.5σ sources in the AzTEC map, where the sampled objects are never closer than one beam size separation, and see how their ACFs compare with the intrinsic ACF of the realization. We test intrinsic ACFs which are strongly and weakly clustered according to power laws of $A_w = 2.9$ and $A_w = 0.5$, respectively, where $\beta = 0.8$. These correspond to values of $r_o \sim 9\,h^{-1}$ Mpc and $r_o \sim 4\,h^{-1}$ Mpc for our assumed redshift distribution function. We again disregard ACF measurements for angular separations smaller than twice the beam size. The purpose of this test is to simulate the ACF we should expect to observe from a map similar to the AzTEC-COSMOS map, if SMGs are intrinsically strongly or weakly clustered galaxies.
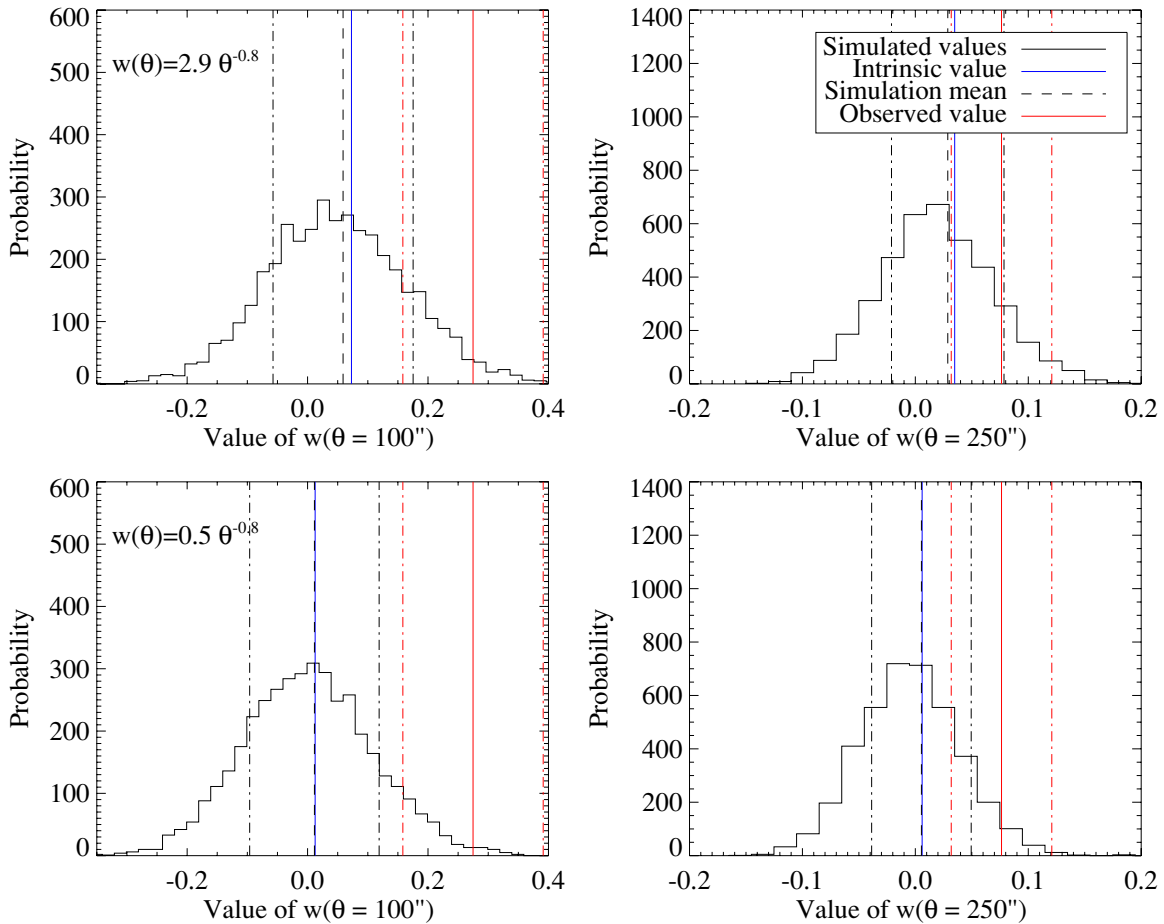
Figure 6. Probability distributions for the ACF at $100''$ and $250''$ separations from the mock catalogs (black histogram). Dashed line is the mean from the mock catalogs, which when corrected for the IC agrees well with the intrinsic value (blue line). Histograms are roughly Gaussian, with standard deviation indicated by dot-dashed lines. Solid red is the observed ACF from the 3.5σ catalog at those angular separations, with Poisson errors given by red dot-dashed lines. Each row results from an intrinsic power-law form shown in the left panel.

In Figure 6, we show the distributions in the value of $w(\theta = 100'')$ and $w(\theta = 250'')$ from the simulations for each power-law form we tested, after applying the correction for false detection rate. The distributions of the ACF values are very broad as should be expected because of the low number of mock galaxies used in each sample, as well as the fraction of random positions. If the measured values are corrected for the integral constraint then the peak of the distributions at each angular separation match well with the intrinsic value. When the distributions are compared to our observation, there is a very small chance of spuriously finding the observed value at $\theta = 100''$ for the 3.5σ sources, about 3% for the strong case and 0.75% for the weak case. At larger separations the chance increases to 31% and 15%, respectively. However, the observed and simulated values for both angular separations for the strong clustering case are consistent within their errors.

We have fit a power law to the mock ACFs, assuming a fixed β of 0.6 or 0.8. The clustering amplitudes we recovered are shown in Figure 7, along with the upper limits we derived from the real AzTEC map. These histograms are essentially probability distributions for clustering amplitudes that will be measured from 189 sources in the AzTEC map area if the intrinsic population is strongly or weakly clustered. In none of the cases explored here is it likely that the intrinsic power-law form will be recovered. The assumed β influences the shape of the distribution, but the probability always peaks at

zero. There is 22% chance that fits assuming $\beta = 0.8$ will indicate zero clustering (24% for $\beta = 0.6$) even if the intrinsic correlation length is $r_o = 9\ h^{-1}$ Mpc. If the intrinsic value is $r_o = 4\ h^{-1}$ Mpc, the percentages increase to 53% and 55% assuming $\beta = 0.8$ and 0.6, respectively. Even though the distributions in Figure 6 nicely correspond with the intrinsic value, the power-law distributions in Figure 7 peak at zero because the large fluctuations in each realization from the small sample size can cause negative values in the ACF. It is not possible to recover the intrinsic clustering properties, and it is not possible to differentiate between strong and weak clustering. The implications this has for millimeter and submillimeter surveys at this resolution and sensitivity, or any survey where such a sparse sampling of the underlying population is detected, are that the true clustering properties cannot be recovered.

4.3. Predictions for Future Surveys

Our sensitivity to the clustering signal in this study is determined by two things. First, the number of sources, which depends on the area mapped and the depth, must be large enough to overcome the high shot noise stemming from the sparse sampling of the underlying galaxy distribution by the SMG selection. Second, the ability to measure small-scale separations between galaxies, which depends on the beam size. Not surprisingly, we generally found that the probability to recover the
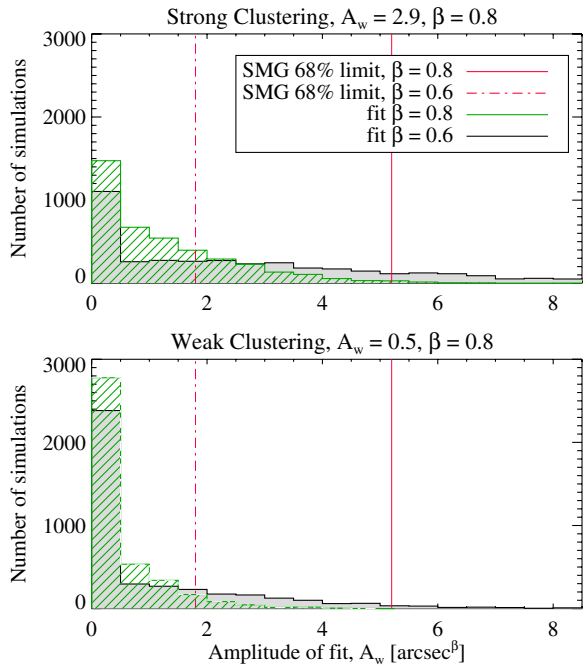
Figure 7. Distributions of clustering amplitudes from fitting power laws to ACFs from clustered simulated maps. Top panel shows results from strong intrinsic clustering ($A_w = 2.9$) and bottom is from weak clustering ($A_w = 0.5$), where $\beta = 0.8$. Green hatched histograms are A_w distributions when fitting with an assumed $\beta = 0.8$, and in gray are assuming $\beta = 0.6$. Red lines are the 68.3% upper limits in A_w from the fit to the ACF of the 3.5σ AzTEC sources, assuming $\beta = 0.8$ (solid red) and $\beta = 0.6$ (dot-dashed red).

Figure 8. Galaxy sample number needed to recover an intrinsic clustering with power-law form $w(\theta) = 2.9\theta^{-0.8}$, as a function of beam size. Area up and left from the contour line indicates region where values may be recovered. Right-hand side axis indicates survey area required at this sensitivity to robustly measure the clustering of the $S_{1.1\,mm} > 4.2$ mJy sources investigated here. Some positions of previous surveys have been provided where possible, based on the source number density of their survey.

intrinsic ACF increases slightly with decreasing beam size; however, the intrinsic value for a sample size such as ours was still not the most likely to be observed down to a beam size of 5″. Increasing the number of detected galaxies, which can be achieved by increasing survey sensitivity or survey area, provides the largest improvement. Fortunately, millimeter and submillimeter facilities are advancing and future studies of SMG clustering will benefit from increased sample sizes and improved angular resolution. Thus the real question becomes, what resolution and survey area will be necessary to get an accurate measure of SMG clustering? Using the strongly clustered simulation discussed in the previous paragraph for an ASTE-COSMOS sized map, we have estimated the limiting galaxy sample size (as a function of beam size) for which it is possible to recover the intrinsic clustering. A measurement of the clustering is considered to have recovered the intrinsic value if, after sampling the parent realization 2000 times and fitting the ACFs, the value of the intrinsic clustering amplitude lies within the standard deviation of the clustering amplitude distribution. Additionally, the distribution must satisfy the requirement that the most likely value of clustering amplitude in the distribution also lies within the standard deviation. This second condition rejects the types of distributions shown in Figures 4 and 7. The resulting "region of robust recovery" is shown in Figure 8. We have added the approximate positions of previous surveys which have made clustering measurements, assuming the estimated number density of detected sources in each is constant. These placements indicate that previously measured ACFs, even the *Herschel* surveys with large area (16 deg²), are still compromised by large beams and low sensitivity. The previous study by Scott et al. (2006), measured from a combination of multiple SCUBA fields, falls within the robust region. However, one caveat of this simulation is that it assumes a contiguous map region. In this case, the signal to
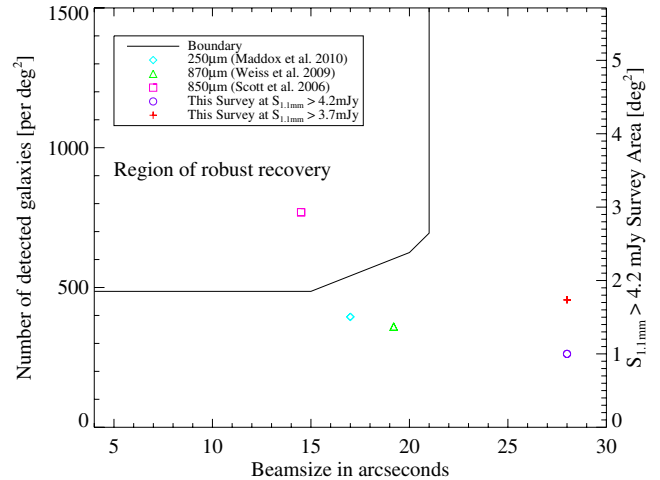
noise of the ACF measurement, which depends on the number of independent galaxy pairs, DD, is related to the total number of detected galaxies N by $DD = 0.5N(N - 1)$. For discontiguous fields, galaxy pairs between fields cannot contribute and so the number of galaxy pairs is lower, given the same number of detected galaxies. For discontiguous identical fields, the number of pairs goes down by a factor of F where F is the number of fields. Thus, measurements made from galaxies in multiple fields will inevitably have lower signal to noise than a measurement using the same number of galaxies from a contiguous area.

The region in Figure 8 illustrates the difficulties in measuring the angular clustering of bright SMGs such as the $S_{1.1\,mm} > 3.7$ mJy samples explored here, but additionally provides some guidance for future surveys which will aim to robustly measure the clustering of SMGs. Upcoming surveys with the Large Millimeter Telescope for example, with its beam size of 6″, will be able to make robust measurements for these galaxies with a mapped area of about 2 deg². These future results will no doubt provide exciting discoveries about the parent population of submillimeter sources.

5. SUMMARY

1. We have measured the angular clustering of SMGs detected at 1.1 mm from the largest contiguous map at that wavelength to date. We have studied sources detected at 3.5σ (3σ) with flux limits $S_{1.1\,mm} > 4.2(3.7)$ mJy. The power-law fits are poorly constrained due to large uncertainties in the ACF.

2. We have set upper limits to the spatial correlation lengths for these galaxies. For flux limits $S_{1.1\,mm} > 4.2$ mJy, we find $r_0 \lesssim 11$–$12\ h^{-1}$ Mpc and for $S_{1.1\,mm} > 3.7$ mJy we find $r_0 \lesssim 6$–$8\ h^{-1}$ Mpc.

3. We have shown that for simulated clustered samples, our map properties, specifically survey area, depth, and beam size, prevent us from accurately measuring strong clustering (e.g., with $r_0 \sim 9\ h^{-1}$ Mpc).

4. We have used these simulations to predict the conditions under which future surveys may robustly detect clustering. Specifically, to measure clustering galaxies detected with $S_{1.1\,mm} > 4.2$ mJy and mapped to a depth of 1.26 mJy beam^{-1},

we will be able to robustly measure clustering with an area of $\sim 2 \deg^2$, with the LMT's beam size of $6''$.

REFERENCES

Adelberger, K. L., et al. 2005, ApJ, 619, 697
Almeida, C., Baugh, C. M., & Lacey, C. G. 2010, arXiv:1011.2300
Amblard, A., et al. 2011, Nature, 470, 510
Austermann, J. E., et al. 2010, MNRAS, 401, 160
Barger, A. J., et al. 1998, Nature, 394, 248
Blain, A. W., Chapman, S. C., Smail, I., & Ivison, R. 2004, ApJ, 611, 725
Brodwin, M., et al. 2008, ApJ, 687, L65
Chapin, E. L., et al. 2009, MNRAS, 398, 1793
Chapman, S. C., Blain, A. W., Smail, I., & Ivison, R. J. 2005, ApJ, 622, 772
Cooray, A., et al. 2010, A&A, 518, L22
Davé, R., et al. 2010, MNRAS, 404, 1355
Eales, S., et al. 1999, ApJ, 515, 518
Giavalisco, M., & Dickinson, M. 2001, ApJ, 550, 177
Hayashi, M., et al. 2007, ApJ, 660, 72
Hughes, D. H., et al. 1998, Nature, 394, 241
Landy, S. D., & Szalay, A. S. 1993, ApJ, 412, 64
Lee, K.-S., et al. 2006, ApJ, 642, 63
Lilly, S. J., et al. 1999, ApJ, 518, 641
Maddox, S. J., et al. 2010, A&A, 518, L11
Negrello, M., et al. 2007, MNRAS, 377, 1557
Peebles, P. J. E. 1980, The Large-scale Structure of the Universe (Princeton, NJ: Princeton Univ. Press)
Porciani, C., & Giavalisco, M. 2002, ApJ, 565, 24
Roche, N., & Eales, S. A. 1999, MNRAS, 307, 703
Scott, K. S., et al. 2008, MNRAS, 385, 2225
Scott, S. E., Dunlop, J. S., & Serjeant, S. 2006, MNRAS, 370, 1057
Scoville, N., et al. 2007, ApJS, 172, 1
Smail, I., Ivison, R. J., & Blain, A. W. 1997, ApJ, 490, L5
Smail, I., Ivison, R. J., Blain, A. W., & Kneib, J. 2002, MNRAS, 331, 495
van Kampen, E., et al. 2005, MNRAS, 359, 469
Viero, M. P., et al. 2009, ApJ, 707, 1766
Webb, T. M., et al. 2003, ApJ, 582, 6
Weiß, A., et al. 2009, ApJ, 707, 1201
Zehavi, I., et al. 2002, ApJ, 571, 172